Transport and Communications Science Journal, Vol. 76, Issue 04 (05/2025), 568-582

Transport and Communications Science Journal

ELECTRICAL RESISTANCE RESPONSE OF A PAIR OF SELF-SENSING CONCRETE BLOCKS UNDER NON-DESTRUCTIVE COMPRESSION

Vo Minh Chi, Nguyen Minh Hai, Nguyen Lan, Pham Van Ngoc*, Nguyen Van Huong, Nguyen Duc Hung

The University of Danang – University of Science and Technology, No 54 Nguyen Luong Bang Street, Danang, Vietnam

ARTICLE INFO

TYPE: Research Article
Received: 27/11/2024
Revised: 15/01/2025
Accepted: 09/05/2025
Published online: 15/05/2025
https://doi.org/10.47869/tcsj.76.4.10

* *Corresponding author*
Email: pvngoc@dut.udn.vn

Abstract. Self-sensing concrete is an advanced material capable of monitoring its stress or strain through changes in its electrical resistance. A novelty of this study lies in its focus on the electrical resistance response, not of an individual concrete specimen as in most previous studies, but rather on a pair of self-sensing concrete blocks under non-destructive compression, targeting future applications in large-scale load-weighing systems. The self-sensing concrete samples in the study were fabricated by incorporating carbon fibers into the concrete mixture, creating a conductive network within the material. The experimental setup involved subjecting a robust steel plate to incremental compressive loads, supported by a pair of self-sensing concrete blocks. The corresponding changes in electrical resistance were measured throughout the loading process. Results indicated that each concrete block might exhibit different responses, but their summed response is nearly linear with a high R-squared value above 0.9 and relatively consistent between experimental cases. Additionally, the study highlighted that variations in the current intensity do not significantly affect the resistance response. On the other hand, the locations of concrete blocks relative to the load were identified as a crucial factor affecting the resistance response. Within the scope of this study, the error in the predicted load value corresponding to the resistance variation when experimental parameters are changed is below 10.7%.The findings of this study demonstrate the significant potential of using self-sensing concrete for large-scale load-weighing systems in future smart traffic and logistics management systems.

Keywords: Self-sensing concrete; double blocks; resistance; non-destructive compression; large-scale weigh station.

1. INTRODUCTION

The development of real-time sensors for monitoring the stress and strain in the structural components, serving the purpose of infrastructure, transportation, and logistics management, is one of the crucial research topics, especially in the context of the vigorous digital transformation happening across most industrial sectors. Currently, various sensor technologies [1], such as fiber optic sensors, piezoelectric sensors, barometric sensors, hydraulic sensors, etc., are widely applied in the construction industry. Despite their advantages, these sensor devices still have certain limitations, such as difficulties in the installation and embedding process over a large area; requiring a large number of sensors to monitor large-scale loads, significantly increasing the cost of the monitoring system; the lifespan of these sensors under environmental factors is not high, and their replacement and repair are relatively complicated and costly [2]. To overcome these drawbacks, the parallel development of new solutions to optimize costs and diversify technology is extremely urgent task.

In this context, concrete capable of sensing its stress and strain (abbreviated as self-sensing concrete) [3] has recently attracted significant interest from the scientific and application communities due to the increasing demand for digital transformation globally. The fundamental principle to creating self-sensing capability in concrete is to introduce conductive materials into the concrete appropriately to increase the conductivity of the concrete to a suitable level [4]. When this is achieved, the characteristic value for conductivity, which is the electrical resistance of the concrete, will vary when the relative positions of the conductive fillers and the internal microstructure of the concrete are altered under mechanical loads such as compression. [5, 6], tension [7], and bending [8]. Therefore, by continuously measuring the variation in the electrical resistance of the concrete, we can indirectly predict the changes in stress or strain within the concrete, thereby calculating and converting these values into load values.

There are various types of conductive fillers used to manufacture self-sensing concrete, including black carbon powder, that are used to manufacture self-sensing concrete [8], carbon fibers [9], steel fibers [8], carbon nanotubes [9], graphene powder [10], nickel powder [11], and others to increase the conductivity of the concrete. Studies by Li et al. [12], Wang et al. [13], and Vaisman et al. [14] indicated that the amount of filler in the concrete significantly affects the concrete's resistance. Research by S. Taheri [15] and T. Shi [16] suggests that the use of conductive fillers such as carbon fibers, carbon nanotubes, and carbon nanofibers should range from 1% to 2% by the volume of the concrete mix. The study by Li et al. [11] suggests that to ensure conductivity within the concrete when using black carbon powder as the filler, the study indicates the amount of filler needs to be designed at a relatively high value, up to 6-7%. Furthermore, when manufacturing self-sensing concrete, using appropriate additives or mechanical treatment methods to disperse the conductive fillers within the concrete is also an essential factor [17]. The ultrasonic solution method is widely used for dispersing nano-sized fillers. Meanwhile, used forced mechanical mixing combined with superplasticizer additives can be applied for larger-sized fibers such as carbon fibers or metal fibers like steel fibers and copper fibers [18].

In addition to fundamental studies on the sensing properties of concrete, numerous studies have focused on developing applications for this material in the construction industry. Rose et al. [19] proposed self-sensing concrete for real-time monitoring of the deformation of

pillar structures and for implementing corrective measures when abnormalities in the concrete's behavior are detected. Francisco et al. [20] utilized self-sensing concrete containing carbon fibers or carbon nanotubes as conductive fillers for beams to monitor deformation behavior. García-Macías et al. [21] and Alessandro et al. [22] proposed the use of concrete as a smart sensor brick embedded in the walls of residential buildings or infrastructure projects for continuous structural health monitoring, particularly for detecting damage following natural disasters such as earthquakes or foundation instability. In the field of infrastructure management and traffic monitoring, Gawel et al. [23] conducted experiments to determine the feasibility of using concrete with conductive fillers embedded in underground concrete pipes to detect water leaks. Han et al. [24] used self-sensing concrete containing carbon nanotubes to detect real-time traffic on different traffic streams, such as vehicle speed and flow. Shi and Chung [25] also used self-sensing concrete for traffic monitoring purposes. In these studies, Weigh-in-Motions (WIM) in smart transportation systems is one of the major significant using self-sensing concrete. However, the studies indicate self-sensing concrete's complex and unstable response under traffic loads. This could be due to (i) the road surface constructed with self-sensing concrete in the form of slabs, where the influence of bending moments on the slab structure complicates the sensor response measurements, and (ii) the dynamic effects of the load make it difficult values to convert and determine vehicle load values accurately.

Given this context, this study aims to develop completely innovative application for self-sensing concrete, which is a large-scale load-weighing system. The basic structure of the weighing system includes multi-sensors made of self-sensing concrete blocks placed underneath a rigid weighing table. In this setup, the load applied to the weighing table is converted into compressive load on the concrete blocks, eliminating the influence of bending moments as in previous studies [24, 25]. Additionally, the stress range studied is within the non-destructive range, meaning that no micro-cracks appear within the concrete during use, thereby extending the lifespan of the weighing system. Initially, this system can be applied as a static weighing system for traffic vehicles or large cargo at ports or industrial warehouses. Later, it can also be optimized for dynamic traffic weighing stations in the future.

In the scope of the initial stage of development, this study aims to clarify the resistance response of self-sensing concrete blocks under compressive stress within the non-destructive range. Thus, the novelty of the study compared to previous studies lies in two core aspects: (i) the resistance response is investigated not only for a single concrete specimen, as in most previous studies, but also for the simultaneous response of a pair of concrete blocks, and (ii) the behavior is examined within the range of small compressive loads, designed to ensure that no microcracks form in the concrete structure. This approach enhances the applicability of this material for repeated use in the actual applications. Additionally, the experimental method allows consideration of the eccentric load effect, bringing the experimental setup closer to the structure of the proposed weighing system. In this study, the self-sensing concrete mix incorporates carbon fibers with a volume content of 2% and is designed to achieve a compressive strength exceeding 50 MPa. Moreover, the study also discusses the effect of the excitation current used during the measurements.

2. MATERIALS AND SPECIMEN PREPARATION

2.1. Raw materials and mix design

Several prior investigations [8-11, 26] have explored the impacts of the type and proportion of conductive fillers on the self-sensing characteristics of concrete. Carbon fiber is

widely recognized as an effective material due to its capacity to form a stable and functional electrical network in the concrete [27] because of its elongated shape and high corrosion resistance. A number of studies [9, 15, 28] typically use carbon fiber contents between 1% and 2% by volume of the concrete mix. Based on the preliminary analyses above, carbon fibers were used in this study with a 2% volume content in the concrete mixture. Moreover, the presence of coarse aggregates can disrupt the continuity of the carbon fiber network, leading to isolated conductive regions within the concrete matrix. As a result, coarse aggregates were excluded from the concrete mix in this study.

Table 1. Properties of raw materials.

Fine sand								
Sieve (mm)		2.36	1.18	0.6	0.3	0.15	<0.15	Total
Retained mass(g)		0	0	21.5	595.5	330.2	52.9	1000.1
Mass percent (%)	0	0	2.15	59.5	33.02	5.29	100	
	0	0	2.15	61.7	94.71	100	-	
FM = 1.58; D_{max} = 0.6 (mm); γ_{os} =1.43 (g/cm^3); γ_{as} =2.43 (g/cm^3) **Notes**: FM is Finess modulus; D_{max} is maximum diameter; γ_{os} and γ_{as} are the unit mass and density of sand.								
Carbon fiber D_f = 7-10 (μm); f_{tf} = 3.6-3.8 (GPa); E_f = 220-240 (GPa); δ_f=1.5 (%); γ_{af}=1.76 (g/cm^3) **Notes**: D_f is the diameter; f_{tf} is the tensile strength; E_f is the tensile modulus; δ_f is the elongation; γ_{af} is the density of carbon fiber.								
Ground Granulated Blast-furnace Slag (GGBS) Chemical composition (%): SiO_2=35.8; Al_2O_3=13.0; CaO=40.2; MgO=7.74; Others=3.26 γ_{aGGBS}=2.89 (g/cm^3); FB_{GGBS} = 5332 (cm^2/g) **Notes**: γ_{aGGBS} is the density; FB_{GGBS} is the fineness blaine of ground granulated blast-furnace slag.								
Superplasticizer Appearance: Liquid, Main chemical ingredients: Polycarboxylate base Dry material content: 25.1 (%); Content: 1.07 (g/cm^3); Chloride content: 0.02 (%).								
Silica Fume (SF) Chemical composition (%): SiO_2=93; SO_3=0.42; CaO=0.62 γ_{aSF}=2.89 (g/cm^3); FB_{SF} = 2580 (cm^2/g) **Notes**: γ_{aSF} is the density; FB_{SF} is the fineness blaine of silica fume.								

Table 1 provides the mechanical and chemical properties of the raw materials for the mixture. Ordinary Portland cement PC50 from Nghi Son Cement JSC, Vietnam, was selected for all test specimens. The natural fine sand used in this study is extracted from a sand quarry located in Hue province, Vietnam, and is predominantly composed of quartz with over 98% content. The majority of the sand particles fall within the size range of 0.3 - 0.15 mm, while particles larger than 0.6 mm and smaller than 0.15 mm are present in minor proportions as shown in Table 1. The carbon fibers are supplied by Haining Anjie Composite Material Co., Ltd., with the basic properties provided by the manufacturer as shown in Table 1. Ground Granulated Blast-furnace Slag (GGBS) and superplasticizers are employed to increase the workability of the concrete mix and enhance the environmental friendliness of the material. The GGBS provided by Hoa Phat Dung Quoc Steel JSC improves the workability of the concrete mixture due to its round shape and smooth surface. Moreover, GGBS contributes to improving the paste's coverage around fine particles, which helps reduce internal friction and enhances the workability of the concrete mixture [29]. A superplasticizer, Lotus-301M, manufactured by Lotus Chemicals JSC, is utilized to improve the workability of fresh mortar

and facilitate better dispersion of fibers within the concrete mixture. In addition, the study includes the use of high-reactivity silica fume (SF), also produced by Lotus Chemicals JSC, as a mineral admixture to boost the strength and durability of the concrete through its pozzolanic properties. The proportions of the concrete mixture, aimed at achieving a target compressive strength of 50 MPa, are shown in Table 2, ensuring suitability for a broad range in actual applications.

Table 2. Mixture proportion for 1m^3 concrete.

Cement (kg)	Silica Fume (kg)	GGBS (kg)	Fine sand (kg)	Carbon fibers (kg)	Superplasticizers (kg)	Water (kg)
480	60	360	1001	14	9	300

2.2. Specimen preparation

Specimens' mixing and pouring process is based on the fabrication method for self-sensing concrete referenced in previous studies [26] as shown in Figure 1(a). The carbon fibers are first divided into small portions and introduced into the concrete mixer along with cement, fine sand, silica fume, and GGBS. The dry mixing is carried out for 2 minutes to ensure thorough blending of the materials. Next, a pre-mixed solution of water and superplasticizer is added to the mixture in three times, with the mixture being wet-mixed for 2 minutes following each addition.

After mixing, the concrete is manually poured into the prepared formwork. Vibration is applied in two stages using a hammer and a vibrating table for 30 seconds at a frequency of 50 Hz. Test specimens without electrodes are prepared to assess the compressive strength of the concrete after 28 days, while other specimens are fitted with copper electrodes, as shown in Figure 1(b), immediately following pouring. The concrete specimens have dimensions of 50x50x250 mm, with the copper electrodes measuring 25 mm in width and 1.0 mm in thickness. The distance between the two electrodes is 20 mm. One day after casting, all specimens are removed from the molds and placed in a curing bath with water for 27 days. Following this, the specimens are cured in a drying oven until their mass stabilizes and reaches zero moisture content, after which resistance measurements are conducted.

It should be noted that, the specimen length of 250 mm was designed based on the size limitations of the loading machine's bearing table, while the sample width of 50 mm was designed to match the capacity of the loading machine to generate a 10 MPa stress while simultaneously loading multiple specimens. It should be noted that, although the rectangular box-shaped samples were intentionally designed to resemble the shape of concrete bearing blocks installed beneath road pavements in large-scale weighing systems, the length-to-width ratio and the dimensions of the electrodes may differ from the actual structures. Moreover, the effect of concrete block dimensions on electrical resistance response under compressive stress has already been clarified in previous studies of the authors [5]. Therefore, the experimental results derived from this study represent general principles, including the simultaneous behavior of a system consisting of multiple concrete bearing blocks as well as the influence of electric currents on this behavior, but they cannot be used to derive generalized formulas for directly applying to the behavior of systems in actual structures. This means that, for each specific weighing system, calibration works of the coefficients representing the relationship between load and resistance changes prior to service is mandatory.

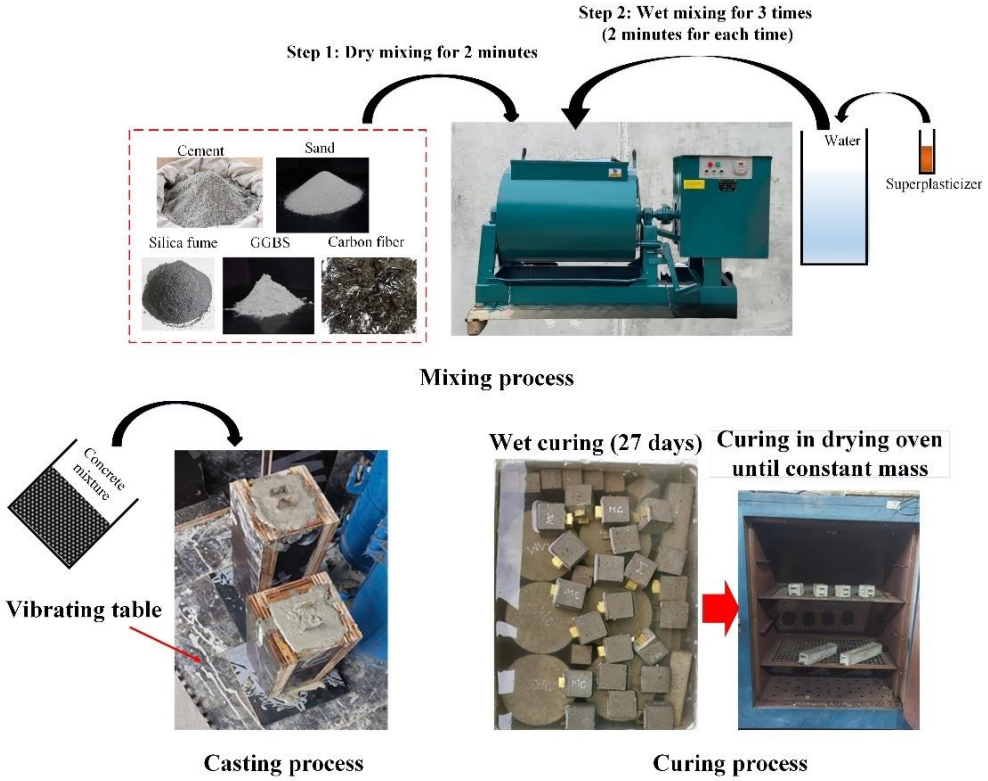

(a) Mixing, poring and curing process of specimens

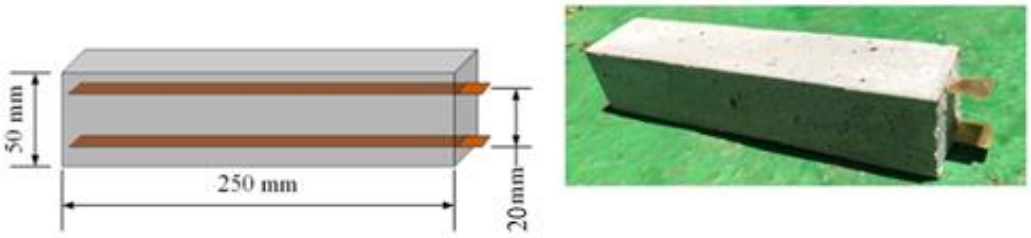

(b) Dimensions of self-sensing concrete block

Figure 1. Specimen preparation of self-sensing concrete block.

3. TEST METHODS AND MEASUREMENT PRINCIPLE

3.1. Test methods

First, the workability of the self-sensing concrete mix was tested using the flow slump test according to ASTM [30]. Additionally, self-sensing concrete samples without electrodes were used to determine the 28-day compressive strength following EN procedures [31]. Meanwhile, concrete blocks with attached electrodes were used in experiments to measure the variation in resistance under load, as shown in Figure 2. In the experiment, a pair of self-sensing concrete blocks was placed under a strong steel plate with a thickness of 30 mm, a width of 290 mm, and a length of 600 mm. This steel plate was used as a table to bear compressive loads. The system was placed on another steel plate of similar dimensions, as shown in Figure 2.

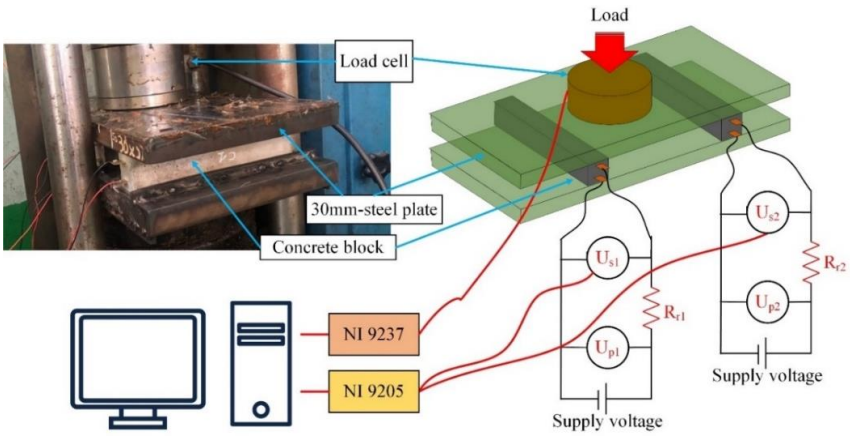

Figure 2. Experimental diagram.

The load was applied to the scale through a load cell placed at the center, allowing for continuous load measurement during the loading process. The loading speed ranged from 0.2 MPa/s to 1.0 MPa/s, and each experiment was repeated two times for reproducibility. The load was applied within the range of less than 1/5 of the target compressive strength of the test samples, meaning below 10 MPa. Within this range, no deformation or cracks were observed in the samples before and after each loading test, allowing them to be used multiple times in experiments to vary different parameters. It should be noted that embedding the copper plate as an electrode into the concrete may alter the stress distribution at the cross-section it occupies due to its elastic modulus being different from that of the surrounding concrete, potentially causing localized damage in the specimens. However, since the stress range is small and the copper plate is very thin (1 mm), this effect can be considered negligible in this study. This assumption is further supported by the high repeatability of the experimental results, as presented in the later sections of the study.

During the loading process, the electrodes of the pair of samples were connected to two independent circuits, as shown in Figure 2. Specifically, each sample was connected in series with a fixed resistor of 50 Ohms and a power rating of 5 W. Each circuit was powered by an independent excitation source using the Instek SPD-3606 power supply, capable of providing a stable voltage range of 1-30V. The load cell was connected to the National Instruments NI-9237 reader, and the NI-9205 reader continuously monitored the Us voltages. The data from both readers were then processed and converted into a digital format using NI Signal Express - 2015 software. The experiment process in Figure 2 was conducted multiple times with varying experimental parameters, including the source voltage and the distance between the pair of blocks.

3.2. Measurement principle

In each circuit in Figure 2, the self-sensing concrete block is considered a resistor (R_s) and is connected in series with an intermediate resistor with a constant value (R_r). By measuring the supply voltage (U_p) of the circuit and the voltage (U_s) between the two R_s electrodes, the resistance between these electrodes of the Self-sensing concrete block can be calculated using the principle below.

The same electric current passes through both as resistor Rs is connected in series with resistor Rr. The total voltage of the circuit is the sum of the voltage drops across R_s and R_r. Equation (1) follows Ohm's law [28] as follows.

$$I(n) = I_s(n) = I_r(n) = \frac{U_s(n)}{R_s(n)} = \frac{U_r(n)}{R_r} = \frac{U_p(n) - U_s(n)}{R_r} \quad (1)$$

in which I(n), $I_s(n)$, and $I_r(n)$ are the current passing through the entire circuit, R_s and R_r, respectively, at the compression loading step n; $U_s(n)$ and $U_r(n)$ are the voltages between the two electrodes of R_s and R_r at the compression loading step n, respectively; $R_s(n)$ is the resistance of the Self-sensing concrete block at the loading step n under specific compressive stress; R_r is the constant intermediate resistor value. Using equation (1), the value of $R_s(n)$ for the Self-sensing concrete block at loading step n can be calculated using equation (2) as follows.

$$R_s(n) = R_r \frac{U_s(n)}{U_p(n) - U_s(n)} \quad (2)$$

When a specific compressive load P(n) is applied to the steel plate during loading step n, the resulting resistance value can be calculated using equation (2). As a result, the change in resistance of each self-sensing concrete block at loading step n, relative to its initial resistance $R_s(0)$ when no compressive stress is applied, can be determined by the value $\Delta R_s(n)$ as follows.

$$\Delta R_s(n) = R_s(n) - R_s(0) \quad (3)$$

On the other hand, since a pair of blocks were used in the experiment, the resistance change values for these two samples are assumed to be ΔRs1(n) and ΔRs2(n), respectively. Therefore, the resistance change value of the system under load can be calculated as the sum of the changes in both blocks, which means

$$\Delta R_s(n) = \Delta R_{s1}(n) + \Delta R_{s2}(n) \quad (4)$$

4. RESULTS AND DISCUSSIONS

4.1. Compressive strength and initial resistance of self-sensing concrete blocks

The results of the spread value according to the flow slump test of the self-sensing concrete mix with carbon fibers used in the study were determined to be 287 mm. In addition, the compression test results indicate that the average compressive strength of the three 28-day-old test samples is 58.4 MPa, exceeding the concrete's designated design strength. Additionally, the blocks were dried to a constant weight and cooled to room temperature before measuring their initial resistance using a handheld ohmmeter. The results showed resistances of 11 and 13 Ohms for the two self-sensing concrete blocks, respectively. This indicates that despite being prepared to the same concrete mixture, there is a slight variation in resistance among the samples due to the impracticality of producing identical samples, as previously demonstrated in the prior study [26].

Next, Figure 3 illustrates the resistivity response when connected to an electrical circuit similar to Figure 2 in an unloaded condition. The ΔRs1 line and ΔRs1 line represent the resistivity response of the 1 and 2's block concrete, while the ΔR_s line depicts the total variation of both blocks according to formula (4). The results show that the resistivity response does not follow any specific pattern, with resistance variation values being negligible, below 0.02 Ohms, and can be disregarded. This demonstrates that the resistivity of the concrete blocks, when provided with an excitation voltage, remains nearly unchanged in the absence of load.

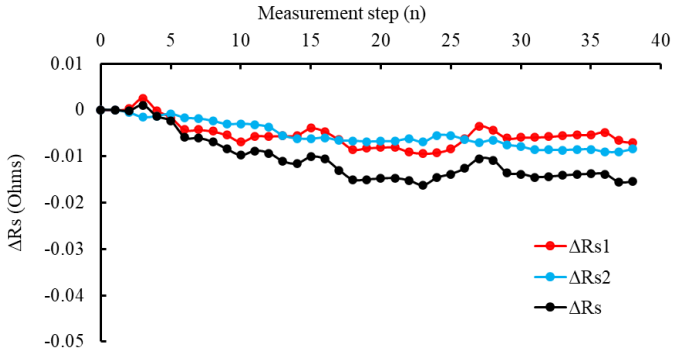

Figure 3. Resistance response of self-sensing concrete blocks under no-load conditions.

4.2. Resistance response under non-destructive compressive load with different locations of self-sensing concrete blocks

Figure 4 shows the electrical resistance response of self-sensing concrete blocks under the compressive load on the weighing table. The lines marked in ΔRs1 and ΔRs2 respectively represent the responses of 1 and 2 block concrete, while the ΔRs line represents the summed response of the two blocks according to formula (4). Figure 4(a) illustrates the case when the two blocks are placed with a center distance of 150mm, with the left and right figures showing the results of the first and second measurements, respectively. Similarly, Figure 4(b) shows the results of the two measurements in the case where the distance between the two blocks is 450mm. In both cases, the excitation voltage source is 10V, corresponding to current intensities of 0.164 and 0.159 A through blocks 1 and 2. Additionally, the maximum applied load for each measurement is 100 kN, corresponding to a calculated stress of 8 MPa generated on the concrete, less than 1/5 of the design compressive strength of the concrete. Within this stress range, due to the absence of microcracks in the concrete, the resistive response of concrete specimens under centrally applied compressive loads is nearly linear, as demonstrated in previous studies [5]. Therefore, linear regression analysis is also applied to the summed response in this study to clarify its linearity under eccentric compressive loading and to examine the stability of the slope coefficient in the relationship between load and resistance when experimental parameters are varied.

Figure 4(a) shows a clear trend where the resistance of the concrete blocks decreases with increasing compressive load, contrasting with the unstable response in Figure 3 when there is no load. This is consistent with the nature of self-sensing concrete, where the conductive components move closer together, and the pore size reduction effect causes a decrease in the resistivity of the concrete blocks under compressive loads. However, the responses of the two self-sensing concrete blocks differ, and these responses are not consistent between the two times of measurement. This is understandable because, even with the same concrete mixture composition, the microstructures of the two blocks cannot be identical. Additionally, although the two blocks were placed symmetrically relative to the load position, the errors in the surface flatness of the concrete blocks and the steel plates can affect the uneven stress distribution between the two samples and between different times of measurements. Here, a fascinating and essential finding is that the black line for both measurements shows a relatively consistent response. The black dotted line represents the regression line of the data points in the summed response of the two blocks, showing that the line slope between the first and second measurements is -0.0023 and -0.0022, respectively, which are quite similar. Furthermore, although the response lines of blocks 1 and 2 show more complex trends, their

summed response exhibits a linear and relatively stable behavior. This is reflected in the correlation coefficient R^2, which is greater than 0.99 for both measurement times. This result indicates that when the steel plate is placed on two self-sensing concrete blocks, although the response of each block under load may differ, their total response is preserved, meaning that for a given applied load, the total change in resistance remains constant.

Figure 4(b) shows a similar response where the distance between the two concrete blocks is 450 mm. The trend is quite similar to that in Figure 4(a), meaning the responses of the two concrete blocks are different and vary between the two measurements. The slopes of regression lines of the total response data are -0.0026 and -0.0023, which are quite similar to the results in Figure 4(a) but slightly higher. However, there is a distinct difference between the results in Figure 4(b) and Figure 4(a), which is the response of the black line, especially in the first measurement, which becomes nonlinear instead of linear. This could be due to the increased distance between the two concrete blocks, causing the effect of eccentric loading to become more pronounced, as shown in Figure 5. This means that the deflection of the steel plate increases, causing the compressive stress applied to the concrete block to become uneven, thereby increasing the nonlinearity of the resistance response of the self-sensing concrete block. This can be considered the influence when an eccentric compressive load acts on a self-sensing concrete block. To reduce this influence, increasing the flexural rigidity of the weighing table and increasing the flat surface area of the concrete blocks can be seen as necessary methods.

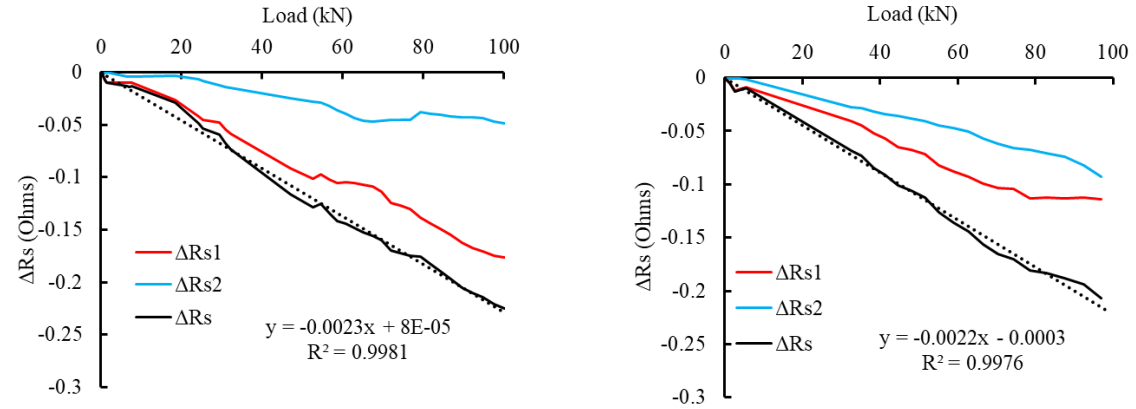

First measurement Second measurement

(a) 150 mm-distance between blocks (U_p = 10V)

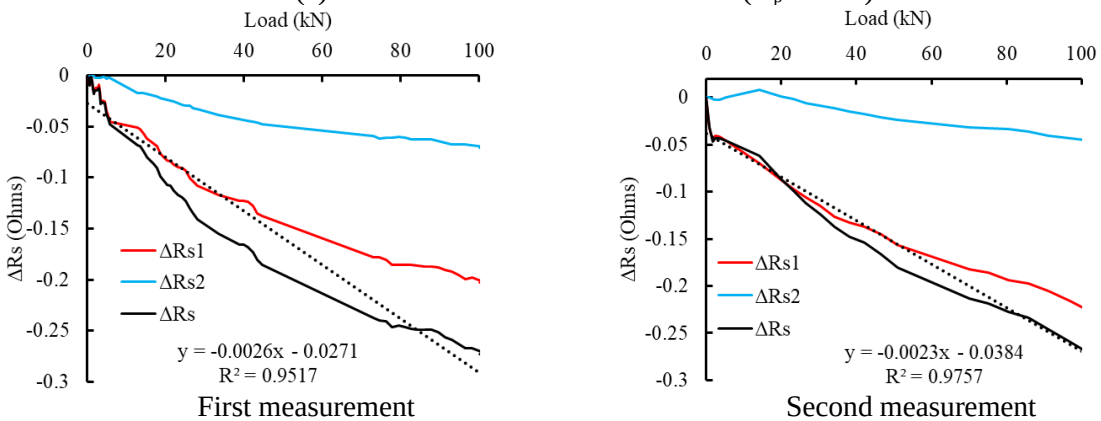

First measurement Second measurement

(b) 450 mm-distance between blocks (U_p = 10V)

Figure 4. Resistance response of self-sensing concrete blocks under compressive load

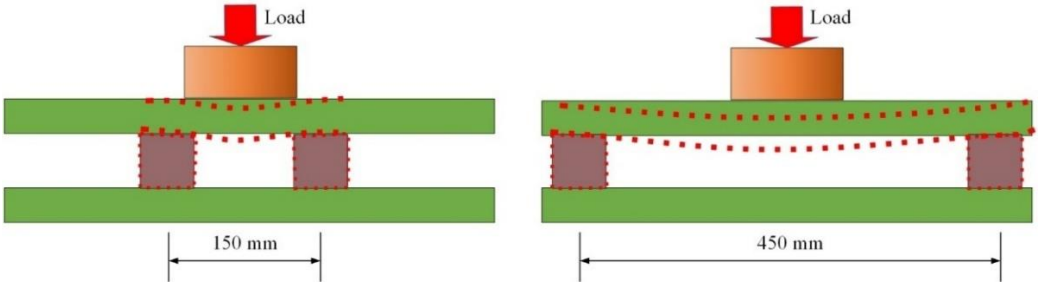

Figure 5. Image of the effect of distance of concrete blocks.

4.3. Resistance response of self-sensing concrete blocks under non-destructive compressive load with supplied voltage

The results in Figure 4 lead to the subsequent experiments that should be conducted with the self-sensing concrete blocks spaced 150 mm apart. The source voltage (Up) is varied in 4 additional cases, including 6, 12, 15, and 18 V, to change the current intensity through the concrete sample, which is one factor that can affect the concrete's resistance response. The measurement results of the resistance response of the concrete samples for these cases are shown in Figures 6(a) to 6(d), respectively. The findings indicate that the responses in these figures show no significant difference compared to the responses explained in Figures 4(a) and 4(b) when the source voltage Up = 10 V. Although the response of each concrete block may be unstable, the overall response is nearly linear and stable in all cases. Varying the source voltage within the 6 – 18 V range changes the current intensity through the sample. However, even at the lowest voltage case of 6V, the current intensity through the sample still reaches 0.098 and 0.095 A. Meanwhile, previous studies have shown that setting the stimulation current intensity above 2 mA stabilizes the resistance behavior of the self-sensing concrete under various loads [5, 6]. Therefore, the current intensity set in this study fully meets this criterion, and increasing the current intensity further results in negligible changes in the resistance response of the concrete samples.

On the other hand, in the application of large-scale load weighing systems, as mentioned in this study, the slope coefficient of the regression line of the summed response, also known as the resistance variation coefficient, is considered a core value for converting the value of resistance variation of the self-sensing concrete blocks in the system into the load value acting on the weighing table. Therefore, determining this value to assign to each product as a calibration value before they are commercialized is essential. Thus, the core technique here is how to minimize the error in this value as much as possible. Figure 6(e) shows the relationship between the slope coefficient of the regression line for the overall resistance response and the source voltage from the measurement results of this study. The box plot illustrates the variation amplitude across two measurement instances, with the cross mark representing the average value of the two measurements. The specific results are also presented in the statistical table within the figure, including the maximum (Max), minimum (Min), average values (Ave), and the percentage ratio between the standard deviation and the average value (SD/Ave, %). The results indicate that the average value in all cases is quite consistent, ranging from -0.0024 to -0.0025. Meanwhile, considering the values of the two measurement ranges, the coefficients vary from -0.0022 to -0.0027, while the mean error fluctuates below 10.7%. These results indicate that although the trend of the experimental results is relatively clear, there is still a specific error in the coefficient of the summed resistance response of the pair of concrete blocks. Figure 7 more clearly shows the measurement error in the study by displaying the set of data points of the summed response

according to the measurement cases, with the orange-colored area representing the data variation range. It can be seen that the upper and lower bounds of the resistance variation coefficient are -0.0022 and -0.0027 compared to the average coefficient of -0.00245. This means that the load value can deviate by ±10.6% from the average predicted value for a given resistance variation value. Therefore, reducing this deviation range is one of the significant challenges in the following research phase for developing advanced large-scale load weighing systems using self-sensing concrete.

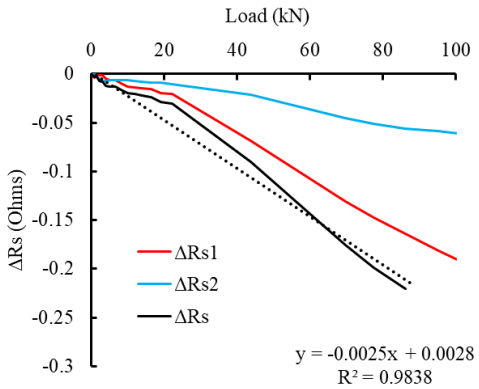

(a) Up = 6 V

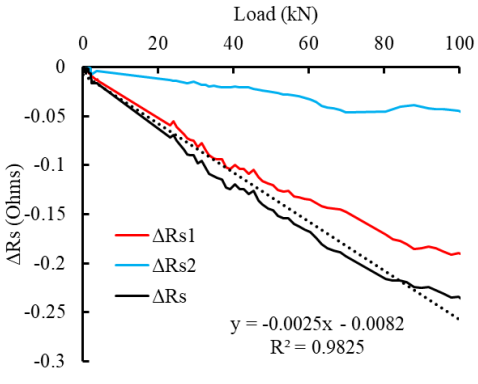

(b) Up = 12 V

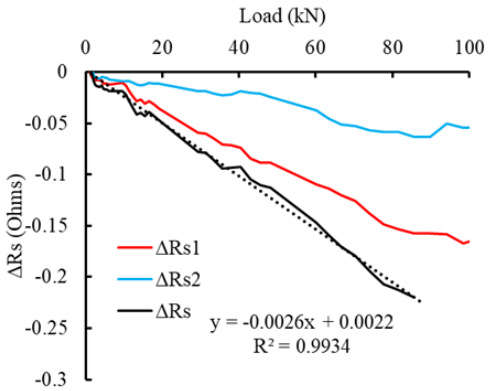

(c) Up = 15 V

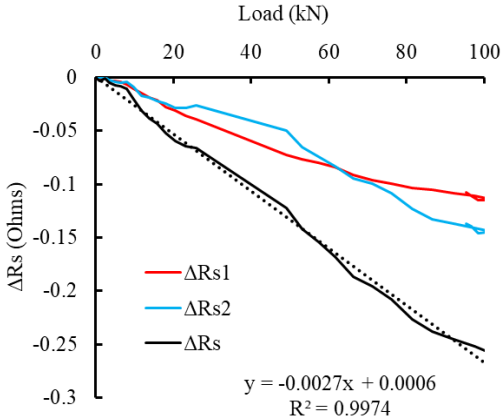

(d) Up = 18 V

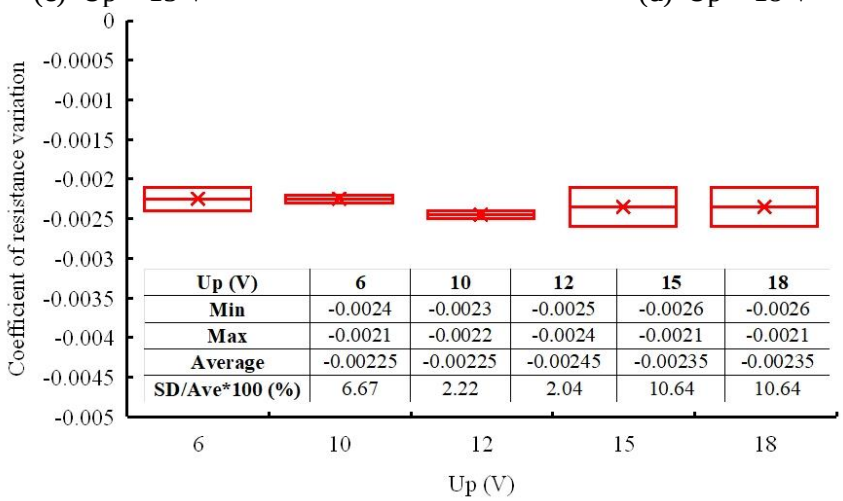

Up (V)	6	10	12	15	18
Min	-0.0024	-0.0023	-0.0025	-0.0026	-0.0026
Max	-0.0021	-0.0022	-0.0024	-0.0021	-0.0021
Average	-0.00225	-0.00225	-0.00245	-0.00235	-0.00235
SD/Ave*100 (%)	6.67	2.22	2.04	10.64	10.64

(e) Relationship of U_p and the coefficient of resistance variation

Figure 6. Resistance response of self-sensing concrete blocks under compressive load.

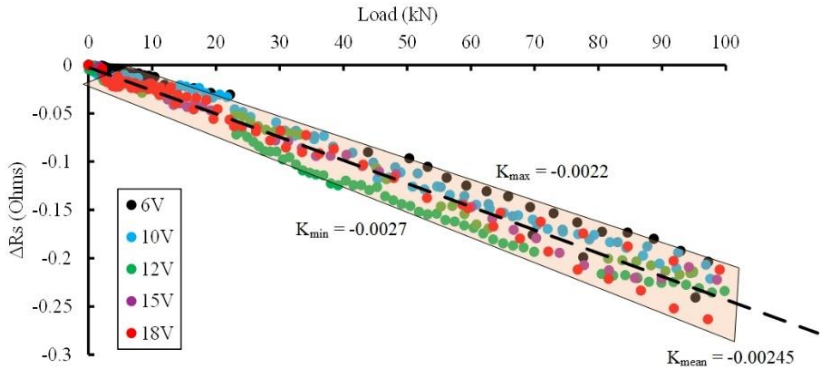

Figure 7. Range of measurement data of the relationship between resistance variation and compressive load.

5. CONCLUSIONS

This study focuses on the electrical resistance response of a pair of self-sensing concrete blocks under non-destructive compression, targeting future applications in large-scale load-weighing systems. The self-sensing concrete samples in the study were fabricated by incorporating carbon fibers into the concrete mixture, creating a conductive network within the material. The experimental setup involved subjecting a robust steel plate to incremental compressive loads, supported by a pair of self-sensing concrete blocks. The corresponding changes in electrical resistance were measured throughout the loading process. The findings from the study are summarized as follows:

(1) The electrical resistance of the self-sensing concrete blocks decreases clearly under the effect of compressive loads within the range under 1/5 of the designed compressive strength of the concrete.
(2) When two concrete blocks are placed under a steel plate receiving compressive loads, the electrical resistance response of each block may differ, but summed response is almost consistent across measurements. This is a significant result demonstrating the potential of this concept for large-scale load-weighing systems.
(3) When the current intensity of the electrical circuit used in the measurements exceeds about 0.09 A, the current intensity does not affect the combined resistance response.
(4) The combined resistance response is nearly linear when the two samples are placed close together and becomes gradually nonlinear as they are placed farther apart. This can be considered the influence when an eccentric compressive load acts on a self-sensing concrete block.
(5) Within the scope of this study, the error in the predicted load value corresponding to the resistance variation is around 10.7%. Therefore, reducing this deviation range is one of the significant challenges in the following research phase for developing advanced large-scale load weighing systems using self-sensing concrete.

However, this study still has some limitations. First, the error in the slope coefficient of the linear relationship between the load and the change in electrical resistance remains at approximately 10%, and this needs to be improved before practical applications can be implemented. Furthermore, the experiments were conducted based on a model consisting of a rigid plate supported by a pair of self-sensing concrete blocks. In actual weighing systems, more than two samples may be used depending on the size of the weighing tables. Therefore, clarifying the summed response of systems with more than two concrete bearing blocks is also an important research direction for the future.

ACKNOWLEDGMENT

This work was supported by Murata Fund and The University of Danang, University of Science and Technology, code number of Project: T2024-02-08MSF.

REFERENCES

[1]. M. Adresi, M. Abedi, W. Dong, M. Yekrangnia, A review of different types of weigh-in-motion sensors: State-of-the-art, Measurement, 225 (2023) 114042. https://doi.org/10.1016/j.measurement.2023.114042
[2]. S. Taheri, A review on five key sensors for monitoring of concrete structures, Construction and Building Materials, 204 (2019) 492-509. https://doi.org/10.1016/j.conbuildmat.2019.01.172
[3]. P.-W. Chen, D.D. Chung, Carbon fiber reinforced concrete for smart structures capable of non-destructive flaw detection, Smart Materials and Structures, 2 (1993) 22-30. https://doi 10.1088/0964-1726/2/1/004
[4]. Z. Tian, Y. Li, J. Zheng, S. Wang, A state-of-the-art on self-sensing concrete: Materials, fabrication and properties, Composites Part B: Engineering, 177 (2019) 107437.
[5]. M.C. Vo, M.H. Nguyen, L. Nguyen, V.H. Nguyen, Stress Self-sensitivity of Carbon Black-filled Mortar under Nondestructive Compression and the Effects of Electric Circuit and Specimen Dimensions, Journal of Advanced Concrete Technology, 21 (2023) 762-776.
[6]. H.V. Le, M. K. Kim, S.U. Kim, S.-Y. Chung, D.J. Kim, Enhancing self-stress sensing ability of smart ultra-high performance concretes under compression by using nano functional fillers, Journal of Building Engineering, 44 (2021) 102717. https://doi.org/10.1016/j.jobe.2021.102717
[7]. D.L. Nguyen, J. Song, C. Manathamsombat, D.J. Kim, Comparative electromechanical damage-sensing behaviors of six strain-hardening steel fiber-reinforced cementitious composites under direct tension, Composites Part B: Engineering, 69 (2015) 159-168. https://doi.org/10.1016/j.compositesb.2014.09.037
[8]. Y. Ding, G. Liu, A. Hussain, F. Pacheco-Torgal, Y. Zhang, Effect of steel fiber and carbon black on the self-sensing ability of concrete cracks under bending, Construction and Building Materials, 207 (2019) 630-639. https://doi.org/10.1016/j.conbuildmat.2019.02.160
[9]. F. Azhari, N. Banthia, Cement-based sensors with carbon fibers and carbon nanotubes for piezoresistive sensing, Cement and Concrete Composites, 34 (2012) 866-873. https://doi.org/10.1016/j.cemconcomp.2012.04.007
[10]. S. Wang, A. Singh, Q. Liu, Experimental study on the piezoresistivity of concrete containing steel fibers, carbon black, and graphene, Frontiers in Materials, 8 (2021) 652614.
[11]. B. Han, K. Zhang, X. Yu, E. Kwon, J. Ou, Nickel particle-based self-sensing pavement for vehicle detection, Measurement, 44 (2011) 1645-1650.
[12]. H. Li, H.-g. Xiao, J.-p. Ou, Effect of compressive strain on electrical resistivity of carbon black-filled cement-based composites, Cement and Concrete Composites, 28 (2006) 824-828.
[13]. H. Wang, X. Gao, R. Wang, The influence of rheological parameters of cement paste on the dispersion of carbon nanofibers and self-sensing performance, Construction and Building Materials, 134 (2017) 673-683. https://doi.org/10.1016/j.conbuildmat.2016.12.176
[14]. L. Vaisman, H.D. Wagner, G. Marom, The role of surfactants in dispersion of carbon nanotubes, Advances in colloid and interface science, 128 (2006) 37-46. https://doi.org/10.1016/j.cis.2006.11.007
[15]. S. Taheri, J. Georgaklis, M. Ams, S. Patabendigedara, A. Belford, S. Wu, Smart self-sensing concrete: the use of multiscale carbon fillers, Journal of Materials Science, 57 (2022) 2667–2682.
[16]. T. Shi, Z. Li, J. Guo, H. Gong, C. Gu, Research progress on CNTs/CNFs-modified cement-based composites–a review, Construction and Building Materials, 202 (2019) 290-307.
[17]. A. D'Alessandro, F. Ubertini, A.L. Materazzi, S. Laflamme, M. Porfiri, Electromechanical modelling of a new class of nanocomposite cement-based sensors for structural health monitoring, Structural Health Monitoring, 14 (2015) 137-147. https://doi.org/10.1177/1475921714560071

[18]. B. Han, K. Zhang, X. Yu, E. Kwon, J. Ou, Fabrication of piezoresistive CNT/CNF cementitious composites with superplasticizer as dispersant, Journal of Materials in Civil Engineering, 24 (2012) 658-665. https://doi.org/10.1061/(ASCE)MT.1943-5533.0000435
[19]. R.M. Chacko, N. Banthia, A.A. Mufti, Carbon-fiber-reinforced cement-based sensors, Canadian Journal of Civil Engineering, 34 (2007) 284-290. https://doi.org/10.1139/l06-092
[20]. F.J. Baeza, O. Galao, E. Zornoza, P. Garcés, Multifunctional cement composites strain and damage sensors applied on reinforced concrete (RC) structural elements, Materials, 6 (2013) 841-855.
[21]. E. García-Macías, F. Ubertini, Earthquake-induced damage detection and localization in masonry structures using smart bricks and Kriging strain reconstruction: A numerical study, Earthquake Engineering & Structural Dynamics, 48 (2019) 548-569. https://doi.org/10.1002/eqe.3148
[22]. A. D'Alessandro, H.B. Birgin, G. Cerni, F. Ubertini, Smart infrastructure monitoring through self-sensing composite sensors and systems: A study on smart concrete sensors with varying carbon-based filler, Infrastructures, 7 (2022) 48. https://doi.org/10.3390/infrastructures7040048
[23]. K. Gawel, D. Szewczyk, P.R. Cerasi, Self-sensing well cement, Materials, 14 (2021) 2021. https://doi.org/10.3390/ma14051235
[24]. B. Han, X. Yu, E. Kwon, A self-sensing carbon nanotube/cement composite for traffic monitoring, Nanotechnology, 20 (2009) 445501. doi 10.1088/0957-4484/20/44/445501
[25]. Z.-Q. Shi, D.D Chung, Carbon fiber-reinforced concrete for traffic monitoring and weighing in motion, Cement and Concrete Research, 29 (1999) 435-439. https://doi.org/10.1016/S0008-8846(98)00204-X
[26]. M.C. Vo, M.H. Nguyen, L. Nguyen, V.H. Nguyen, An empirical model for electrical resistivity of mortar considering the synergistic effects of carbon fillers, current intensity, and environmental factors, Case Studies in Construction Materials, 19 (2023) e02685. https://doi.org/10.1016/j.cscm.2023.e02685
[27]. J. Han, J. Pan, J. Cai, X. Li, A review on carbon-based self-sensing cementitious composites, Construction and Building Materials, 265 (2020) 120764.
[28]. M. G. Falara, A.K. Thomoglou, F.I. Gkountakou, A. Elenas, C.E. Chalioris, Hybrid smart cementitious materials incorporating ladder scale carbon fiber reinforcement: An experimental investigation, Case Studies in Construction Materials, 18 (2023), e02035.
[29]. H. Feng, S. Nie, A. Guo, L. Lv, L. Chu, J. Yu, Fresh properties and compressive strength of MPC-based materials with blended mineral admixtures, Case Studies in Construction Materials, 17, e01201, 2022. https://doi.org/10.1016/j.cscm.2022.e01201
[30]. A. ASTM, Standard specification for flow table for use in tests of hydraulic cement, ASTM West Conshohocken, 1 (2014).
[31]. B. Standard, Testing hardened concrete, Compressive strength of test specimens, BS EN 12390-3:2009.